Ethacrynic Acid Effects on Inner Wall Pores in Living Monkeys

C. Ross Ethier,[1] Mary Ann Croft,[2] Fides M. Coloma,[1] Ronald E. Gangnon,[3] William Ladd,[3] and Paul L. Kaufman[2]

Purpose. The influence of the inner wall of Schlemm's canal on aqueous outflow facility remains poorly understood. We examined the relationship between inner wall pore characteristics and outflow facility in living primate eyes in which facility had been pharmacologically increased by ethacrynic acid (ECA) infusion and in contralateral control eyes.

Methods. Outflow facility (two-level constant pressure perfusion) was measured in eight pairs of living monkey eyes before and after administration of a bolus dose of either 0.125 mM ECA or vehicle. After exsanguination, eyes were fixed in situ under constant-pressure conditions (mean fixation pressure ≈19 mm Hg). The density and diameter of inner wall pores and the number and area of platelet aggregates on the inner wall of Schlemm's canal were measured by scanning electron microscopy.

Results. In ECA-treated eyes, outflow facility increased 63% ($P < 0.0001$), intracellular pore density decreased 46% ($P = 0.0094$), intracellular pore size increased 27% ($P = 0.049$), platelet aggregate density increased 158% ($P < 0.0001$), and area covered by platelets increased 210% ($P = 0.012$) relative to contralateral controls. Although the average density and size of intercellular pores were essentially unaffected by ECA, an increased density of large (≥1.90 μm) intercellular pores was seen in ECA-treated eyes. The density of intracellular pores increased with the duration of fixative perfusion. Other than a weak negative correlation between outflow facility and intracellular pore density in ECA-treated eyes ($P = 0.052$), facility was not correlated with inner wall pore features.

Conclusions. Our data are most consistent with a scenario in which ECA promotes formation of large intercellular pores in the inner wall of Schlemm's canal, which are then masked by platelet aggregates. Masking of intercellular pores, combined with fixation-induced alteration of inner wall pore density, greatly complicates attempts to relate facility to inner wall structure and suggests that in vivo pore density is smaller than in fixed tissue. Additionally, facility-influencing effects of ECA on the juxtacanalicular tissue cannot be excluded. (*Invest Ophthalmol Vis Sci.* 1999;40:1382-1391)

The precise site of aqueous humor outflow resistance in normal eyes is unknown, as is the cause of increased outflow resistance in primary open-angle glaucoma. Development of new drugs for controlling ocular hypertension would be greatly aided by an improved understanding of factors controlling outflow resistance in normal and glaucomatous eyes. In normal eyes, the bulk of available evidence points to the inner wall of Schlemm's canal and/or the juxtacanalicular tissue as the primary site(s) of aqueous outflow resistance.[1-3] The role of the inner wall of Schlemm's canal remains controversial: Early studies[4,5] indicated that the inner wall is responsible for only a small fraction of outflow resistance. Despite the small resistance *directly* attributable to the inner wall, a number of experiments point to the potential of the inner wall to influence outflow facility *indirectly*. Specifically, numerous studies have shown that disruption of the inner wall is correlated with an increase in outflow facility. This disruption can result from artificially increased intraocular pressure (IOP),[6] cytochalasin-B,[7,8] sulfhydryl-active agents,[9] EDTA,[10] α-chymotrypsin,[11] *N*-ethyl maleimide,[3] or ethacrynic acid (ECA).[12,13] Conversely, it has been shown that outflow facility is markedly reduced after retroperfusion with glutaraldehyde,[3] which presumably acts to "stiffen" the inner wall by cross-linking cell-surface and transmembrane proteins to the underlying matrix. Additionally, recent work indicates that the density of transendothelial pores in the inner wall of Schlemm's canal can depend on factors such as time since death and the details of tissue fixation.[14] It was also shown that there are two types of inner wall pores, and that these pore types respond in different

From the [1]Departments of Mechanical Engineering and Ophthalmology, University of Toronto, Ontario, Canada; and the Departments of [2]Ophthalmology and Visual Sciences and [3]Biostatistics, University of Wisconsin, Madison.

Presented in part at the annual meeting of the Association of Research in Vision and Ophthalmology, Fort Lauderdale, Florida, 1996.

Supported by Grant MA-10051 (CRE) from the Medical Research Council of Canada; Grants EY02698 (PLK) and EY07119 (WL, RG), National Eye Institute, Bethesda, Maryland; Research to Prevent Blindness, New York, New York (PLK); and Telor Ophthalmic Pharmaceuticals, Danvers, Massachusetts (PLK).

Submitted for publication October 18, 1998; accepted January 24, 1999.

Proprietary interest category: Pc, C3,5, Cc3-8 (PLK). None of the authors had any personal proprietary interest, nor did they receive any personal payment or considerations relative to ethacrynic acid or Telor Ophthalmic Pharmaceuticals. PLK served as a paid consultant to Telor on projects unrelated to ECA. Telor contributed to a nonprofit charitable organization for which PLK serves as a nonpaid officer and member of the Board of Directors.

Reprint requests: C. Ross Ethier, Department of Mechanical and Industrial Engineering, University of Toronto, 5 King's College Road, Toronto, Ontario M5S 3G8 Canada.

Investigative Ophthalmology & Visual Science, June 1999, Vol. 40, No. 7

ways to fixation and postmortem effects.[15] It is therefore clear that further study of the physiology of the inner wall is needed to understand better what role (if any) inner wall pores play in determining outflow facility.

One possible mechanism whereby inner wall pores can indirectly influence outflow facility is known as the pore-funneling theory.[16] It predicts that facility should be proportional to the permeability of the juxtacanalicular tissue, K_{JCT}, and to the nD product, defined as inner wall pore density n, multiplied by pore size D. It follows that if K_{JCT} is similar between fellow eyes of a pair, then the ratio of facilities for the fellow eyes is predicted to be proportional to the ratio of nD products for the fellow eyes. Experimental confirmation of such a relationship would lend strong support to the validity of the funneling theory.

One method of studying the possible role of inner wall pores is to administer agents that alter inner wall pore densities and/or sizes and observe the resultant effects on outflow facility. Ethacrynic acid, a sulfyhydryl-reactive diuretic, increases outflow facility in primate eyes in vivo (e.g., Croft et al.,[12] Epstein et al.[17]) and in enucleated human eyes.[18] We have shown that ECA increases outflow facility and inner wall pore density in enucleated human eyes.[13] However, because of the possible confounding effects of time after death, it was desirable to perform a companion study in living eyes. We therefore examined how ECA affects inner wall pores and facility in the living monkey eye, with specific emphasis on relating inner wall pore features to outflow facility and testing the pore-funneling hypothesis. Based on earlier reports[7,19] of platelets adhering to the inner wall under experimental conditions, we also quantified platelet distributions in normal and experimental eyes.

Methods

Perfusion Experiments

Eight adult rhesus monkeys (*Macaca mulatta*), free of anterior chamber (AC) cells and flare or other biomicroscopically visible ocular abnormalities, were anesthetized with 10 mg/kg intramuscular ketamine followed by 35 mg/kg intramuscular pentobarbital sodium. A catheter was placed in a femoral artery, and the AC of each eye was cannulated with one branched needle (inserted superiorly) and one unbranched needle (inserted inferiorly). The branched needle was connected via polyethylene tubing and stopcocks to a continuously weighed reservoir on one branch and a pressure transducer on the other. The unbranched needle was connected to polyethylene tubing that was clamped off. Total outflow facility was measured by two-level constant pressure (AC) perfusion, at approximately 3 mm Hg and 12 mm Hg above spontaneous IOP, with Bárány's mock aqueous humor, correcting for the internal resistance of the perfusion apparatus.[20,21] Spontaneous IOP under pentobarbital anesthesia differed between monkeys, ranging from 6.25 mm Hg to 20 mm Hg. Baseline facility was determined for 45 to 60 minutes, after which the branched needle was closed to inflow. The clamped tubing from the unbranched needle was then connected to syringes containing 0.125 mM ECA drug solution (contents described later) in one eye or vehicle in the contralateral eye, and the fluid in the external reservoirs was exchanged correspondingly. The syringes were placed in a variable speed infusion pump, and the tubing previously leading to the reservoir was opened to air, allowing infusion of 2 ml of drug or vehicle solution through the AC over 10 minutes. During AC exchange, the same IOP was maintained in both eyes of each monkey, with a treated-control IOP difference of only 0.13 ± 0.61 mm Hg (mean ± SEM). However, the IOP differed between monkeys, possibly because of animal-specific differences in the effects of anesthetic agents, and normal interanimal differences in spontaneous IOP. The reservoir was then reconnected but not opened to the eye, and the syringe tubing was again clamped. Thirty minutes after AC exchange, the reservoirs were reopened, and facility was measured for 45 to 60 minutes. This technique[22] allows rapid drug administration, excellent AC mixing, and nearly constant intracameral drug concentration after AC exchange, because the perfusate from the reservoir contains the desired drug concentration during the posttreatment facility measurements.

After the postdrug facility measurements, 2 ml to 3 ml heparin (1000 U/ml) was administered through the femoral artery catheter, and 5 minutes later, exsanguination through the catheter was begun. During exsanguination, the eyes were fixed in situ by a 10-minute AC exchange with 2 ml of fixative solution (4% glutaraldehyde and 4% paraformaldehyde in Sörenson's buffer [pH ~7.3]), as described earlier. During AC fixative exchange, approximately the same IOP was maintained in contralateral eyes, with treated-control IOP differences of −0.58 ± 0.89 mm Hg (n = 6, data for two monkeys not collected); however, IOP differed among monkeys (range, 6–12 mm Hg). After AC exchange with fixative was completed, the eyes were further perfused with fixative for 1 hour at constant pressure. Fixative volume, duration, and pressure were all measured. The fixative perfusion pressure differed slightly among monkeys (mean, 18.8 mm Hg; range, 17–23.25 mm Hg, corresponding to 5–11.9 mm Hg above spontaneous IOP) but was stable during the fixative perfusion period and was matched between fellow eyes. This corresponds to an equal-pressure fixation protocol, as opposed to an "equal-flow" protocol in which fixative flow rate is matched between fellow eyes.[13,14] The animals died (as a result of exsanguination or pentobarbital overdose) 10 to 40 minutes after AC exchange with fixative was complete. After enucleation, a small incision was made in the equatorial region of the globe, with care taken to avoid pressure, and the eyes were further fixed by immersion for at least 24 hours. All experiments were conducted in accordance with National Institutes of Health and institutional guidelines and with the ARVO Statement on the Use of Animals in Ophthalmic and Vision Research.

Drug Preparation

A solution of 0.125 mM ECA (Sigma, St. Louis, MO) was prepared in Bárány's mock aqueous humor[20] containing 1% dimethyl sulfoxide (DMSO; Research Industries, Salt Lake City, UT) by volume, used to solubilize the ECA. This is a near-maximal dose for increasing facility when given by AC exchange (unpublished data). The vehicle solution was Bárány's mock aqueous containing 1% DMSO without ECA. This volume of DMSO in the 100-μl cynomolgus monkey AC[23,24] has no effect on outflow facility[25,26] or AC angle morphology.[7,27] Both solutions were pH-balanced between 7.0 and 7.4 and were made fresh each day.

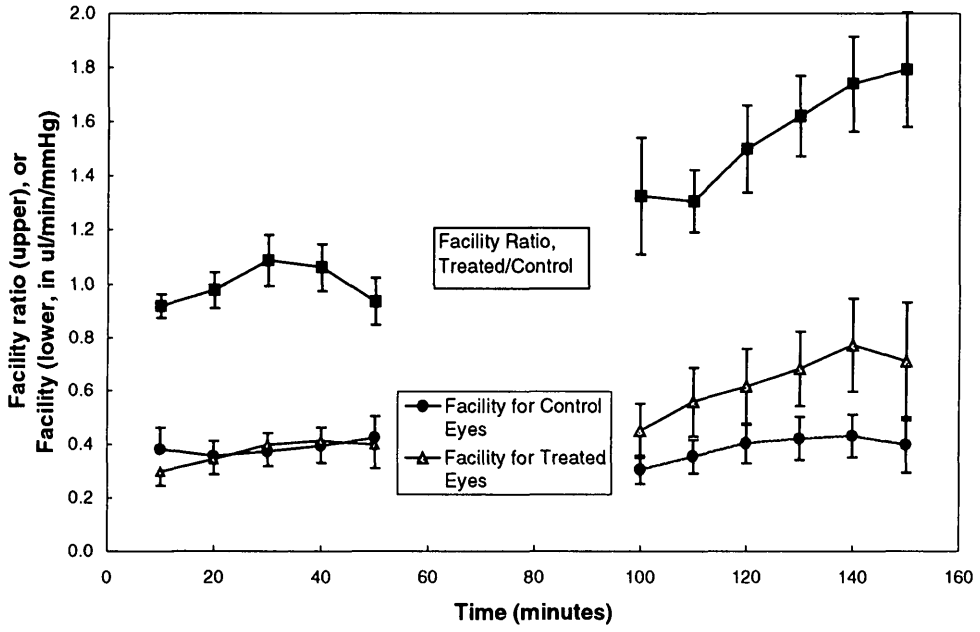

FIGURE 1. Plot of normalized mean facility ratio ($C_{ECA}/C_{contralateral\ control}$; *upper data*) and facility (*lower data*) versus time for eight pairs of monkey eyes. The break in the graph is the 40-minute period (10-minute AC exchange with ECA or vehicle plus 30-minute wait before reopening the external reservoir) during which facility was not measured. Bars are SE. The slope of a line regressed to the normalized facility data before ECA infusion is not significantly different from zero; after ECA infusion, the slope of the regressed line ($r^2 = 0.95$) was 0.011 ± 0.0012 per minute (mean ± SE; $P < 0.001$).

Morphometric Analysis

Pores in the inner wall of Schlemm's canal were morphometrically analyzed after a protocol identical with that previously used for human eyes.[13,14] In brief, all tissue samples were masked, Schlemm's canal was microdissected[14,28] to expose inner wall segments from all quadrants of each eye, and scanning electron micrographic montages (magnification, ×1500) of the inner wall of Schlemm's canal were prepared and used for tentative identification of pores. The original tissue samples were then put back into the scanning electron microscope and re-examined at high magnification (×10000), to exclude artifactual pores. During this procedure, we measured the size of each pore and classified pores according to whether they were intracellular (I pores) or intercellular (B pores). A small percentage (0%-5%) of pores was ambiguous and thus was classified as unknown. The following quantities were recorded for each quadrant: pore density (n: pores per square millimeter) for each of I, B, and unknown pore types; mean pore size (D: in micrometers) for each of I, B, and unknown pore types; and nD, nD^3, and nD^4 products for each of I, B, and unknown pore types. Quantities of the form nD^q (q = 1, 3, 4) were computed using the formula $(\Sigma D^q)/A$, where A is the inner wall area analyzed for that quadrant and the sum extends over all pores of a given type in that quadrant. Whole-eye values were obtained by simple arithmetic averaging of values from individual quadrants, except for pore size D, which was obtained by a weighted averaging procedure accounting for the number of pores seen in each quadrant, D (weighted) = $\Sigma(n_iD_i)/\Sigma n_i$, where the sum index i varies over the number of quadrants analyzed for that particular eye. For some eyes, data were not available from all quadrants because of dissection difficulties.

After analysis of inner wall pores, platelet aggregates adhering to the inner wall were studied. In particular, the number of aggregates and the area of each aggregate were measured from overview montages. Platelets were identified by their approximately spherical shape and size; platelet aggregates were defined to consist of two or more platelets in physical contact with one another. In two pairs of eyes, tissue was further processed for transmission electron microscopy (TEM) by redehydrating the samples in a graded series of ethanols, embedding them in Epon-Araldite, and cutting thick sections on an ultramicrotome (model MT7000; RMC, Tucson, AZ). By using inner wall landmarks when comparing scanning electron micrographic montages and thick sections, it was possible to determine when the microtome was about to section through a platelet clump. In such regions, ultrathin sections passing through platelet aggregates were cut, stained with uranyl acetate and lead citrate, and viewed on a transmission electron microscope (model H-7000; Hitachi, Tokyo, Japan).

Statistical Methods

Statistical analysis was performed using statistical analysis software (SAS Procedure Mixed; SAS, Cary, NC). Analyses of outflow facility and inner wall statistics were based on a linear mixed-effects model for log(response) which included a monkey-specific random effect and a fixed effect for the difference between ECA-treated and control eyes. Estimates were back-transformed (exponentiated) to be on the original scale. Models accounting for differing areas analyzed per eye were considered but not reported. These models yielded inferences comparable to the models presented. The relationships between outflow facility and inner wall features are based on the relationship between the log(response) and the log(predictor), controlling for a fixed drug effect and monkey-specific random effects.

RESULTS

Ethacrynic Acid's Effects on Facility

The mean pretreatment facilities (C_{pre}) were almost identical between control and ECA eyes (0.34 versus 0.33 μl/min · mm Hg Fig. 1). In eyes perfused with vehicle alone, the mean posttreatment facility (C_{post}) was essentially unaffected by perfusion with vehicle. However, ECA perfusion caused a marked increase in aqueous outflow facility in every monkey studied, leading to a mean 56% facility increase in ECA-treated eyes.

TABLE 1. Summary of Drug Effects in Monkey Eyes

	Control	ECA	ECA/Control	*P*
Facility (μl/min/mm Hg)				
C_{pre}	0.34 (0.21-0.57)	0.33 (0.20-0.54)	0.95 (0.80-1.14)	0.5388
C_{post}	0.34 (0.20-0.58)	0.54 (0.32-0.91)	1.56 (1.19-2.03)	0.0056
C ratio (C_{post}/C_{pre})	1.01 (0.86-1.17)	1.65 (1.41-1.92)	1.63 (1.44-1.85)	<0.0001
Inner wall area analyzed per eye (mm^2)	0.14 (0.07-0.28)	0.12 (0.06-0.24)	0.85 (0.62-1.18)	0.2822
Pore density (per mm^2)				
I	740.9 (318.8-1722)	401.3 (172.7-932.8)	0.54 (0.36-0.82)	0.0094
B	86.3 (19.5-382.8)	105.0 (23.7-465.8)	1.22 (0.20-7.44)	0.8050
Total (I+B+U)	863.6 (369.3-2020)	602.2 (257.5-1408)	0.70 (0.40-1.20)	0.1627
Pore size (μm)				
I	1.37 (1.07-1.76)	1.86 (1.44-2.39)	1.36 (1.02-1.80)	0.0380
B	2.01 (1.34-3.01)	2.52 (1.64-3.85)	1.26 (0.82-1.92)	0.2399
Total (I+B+U)	1.45 (1.08-1.94)	2.09 (1.57-2.80)	1.44 (1.01-2.06)	0.0442
nD product (μm per mm^2)				
I	1014 (461-2229)	744 (338-1635)	0.73 (0.44-1.21)	0.1880
B	173 (28-1047)	243 (40-1476)	1.41 (0.18-11.18)	0.7071
Total (I+B+U)	1251 (499-3137)	1260 (502-3159)	1.01 (0.45-2.28)	0.9843
Platelets				
Aggregates per area	218 (92-518)	562 (237-1334)	2.58 (2.02-3.28)	<0.0001
Area covered by	1.38 (0.62-3.04)	4.27 (1.93-9.42)	3.10 (1.41-6.82)	0.0116

Values are means with 95% confidence interval in brackets; $n = 8$ pairs of eyes. Note that the mean (ECA/control ratio) does not equal the (mean ECA)/(mean control) ratio. C_{pre} and C_{post}, facility before and after drug/vehicle infusion, respectively; I, intracellular; B, intercellular; U, unknown type.

When expressed as a net facility ratio (C_{post}/C_{pre} for ECA-treated eyes divided by C_{post}/C_{pre} for contralateral control eyes), the mean facility increase due to ECA was approximately 63% ($P < 0.0001$; Table 1). The facility change after ECA perfusion was gradual and time dependent (Fig. 1), similar to that seen in human eyes.[13]

Inner Wall Pores

In general, the microdissection of Schlemm's canal to expose the inner wall of Schlemm's canal was more difficult in monkey eyes than in human eyes, because of a variety of factors: Compared with human eyes, Schlemm's canal in monkey eyes had more septa, more bifurcations, and a smaller size. As a result, the average inner wall area suitable for pore counting averaged approximately 130,000 μm^2 per eye, which is slightly less than the 200,000 μm^2 per eye previously obtained in a similar study using human eyes.[14] However, it is within the range of areas studied by other investigators (Table 2).

The overall inner wall appearance in monkey eyes was more disordered than in human eyes, with tissue bridges and valleys giving a more three-dimensional topography to the inner wall (Fig. 2; compare with Fig. 2 of the companion human eye report[13]). The inner wall in both control and drug-treated eyes showed spindle-shaped endothelial cells that frequently bulged into the lumen of Schlemm's canal. As in human eyes, there was a great deal of heterogeneity in the topography of the inner wall: some areas were heavily vacuolated, whereas other areas appeared to be almost completely flat. B and I pores with smooth edges were observed in all tissue samples studied (Fig. 2). In general, the qualitative ap-

TABLE 2. Summary of Current and Previously Reported Inner Wall Pore Densities in Control Monkey Eyes

Species	Pore Density (pores/mm^2)*	Mean IW Area Analyzed Per Eye (μm^2)	Fixation Pressure (mm Hg)	Reference
Rhesus	864 ± 249 (n = 8)	146,000	18.6	Present study
Rhesus	1060 ± 431 (n = 3)	100,000	15	Moseley et al.[36]
Vervet and Rhesus	1150 (n = 5)	At least 18,000	Spontaneous IOP	Bill[37]
Cynomolgus	1990 ± 291 (n = 12†)	268,000	18.6	Svedbergh[35]
Cynomolgus and Japanese	1477 ± 434 (n = 2‡)	176,000	At or near spontaneous IOP	Hamanaka and Bill[19]

* Values are means ± SE, with number of eyes shown in parentheses. If SE were not given or could not be computed from original data, only mean and number of eyes are shown.

† Original data interpolated to a fixation pressure of 18.6 mm Hg; SE for pore density is SE reported at 12 mm Hg and n is number of eyes at 12 mm Hg.

‡ Based on control eyes for monkeys A and C. For monkey C, fixation IOP was not reported.[19] However, based on reported details of the experimental protocol, it would appear to be close to spontaneous IOP.

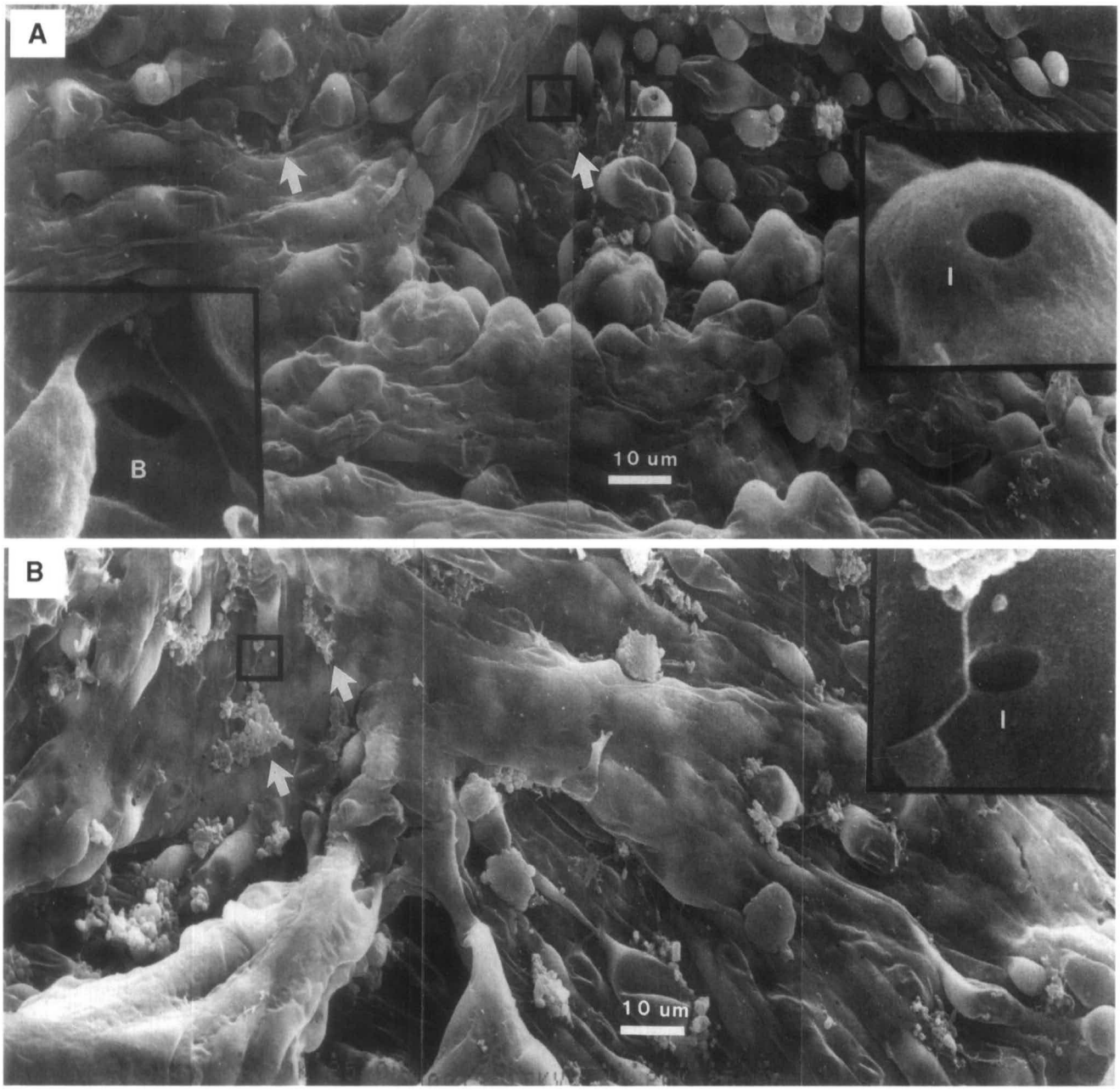

FIGURE 2. Overview SEM montage of control (A) and contralateral ECA-perfused (B) monkey eyes. Insets show high-magnification views of boxed regions surrounding pores. Platelet aggregates (*arrows*) with occasional attached fibrin strands are visible in both panels but are more numerous and larger in ECA-treated eyes. I: intracellular pore; B: intercellular (border) pore.

pearance of inner wall pores was similar to that previously reported for human and monkey eyes. Platelet aggregates were seen adhering to the wall of Schlemm's canal in both control and ECA-treated eyes (Fig. 2). Leukocytes were occasionally seen, whereas red cells were almost entirely absent.

In control eyes, there were approximately 860 pores/mm^2, which is approximately half the pore density seen in fresh human eyes (Table 3). Border (B) pores were in the minority, accounting for only 10% of all identifiable pores, which is a smaller proportion than seen in fresh human eyes. B pores tended to be larger than I pores (Tables 1, 3). This is qualitatively similar to the situation in fresh human eyes; however, in human eyes, mean B and I pore sizes were smaller than those reported here (Table 3).

Considering overall pore densities and sizes, ECA had a marked effect on I pores, but essentially no effect on B pores. Specifically, ECA-treated eyes showed an approximate 46% reduction in the density of intracellular (I) pores ($P = 0.0094$) and a 27% increase in mean I pore size ($P = 0.049$; Fig. 3, Table 1). Conversely, ECA-treated eyes had slightly increased B pore density (by a statistically nonsignificant 22%) and an essentially unchanged mean B pore size (Fig. 4, Table 1). Considering all pores together, the net effect of ECA was a 30% decrease in total inner wall pore density ($P = 0.163$) and a 35% increase in mean pore size ($P = 0.054$).

A slightly different picture of the effect of ECA emerges when individual pore size groupings are considered. Considering only the largest pore size categories ($\geq$1.9 μm), which would

TABLE 3. Comparison of Pore Statistics for Control Monkey Eyes and Fresh Human Eyes (Vehicle Perfusion Only)

	Monkey (n = 8)	Human (n = 13)*
I pores		
Pore density (per mm^2)	740.9 (318.8-1722)	1341 (966.5-1860)
Mean size (μm)	1.37 (1.07-1.76)	0.99 (0.82-1.19)
Percentage of identifiable pores (%)	87.1 (78.6-96.5)	76.0 (67.5-85.6)
B pores		
Pore density (per mm^2)	86.3 (19.5-382.8)	380.0 (265.2-544.6)
Mean size (μm)	2.01 (1.34-3.01)	1.51 (1.33-1.72)
Percentage of identifiable pores (%)	10.1 (5.6-18.2)	21.5% (15.3%-30.4%)

All values are means, with 95% confidence intervals in parentheses; n is number of eyes.

* Human eyes were perfused with mock aqueous humor within 15 hours of death; data were from Ethier et al.[15]

presumably be responsible for the majority of fluid transport across the inner wall, the density of these large I pores was essentially unchanged in ECA-treated eyes (Fig. 3). There was also no statistically significant increase in B pore density (P = 0.17), because the approximate 4-fold increase in mean B pore density in these large size categories was accompanied by large standard deviations in the individual pore size densities (Fig. 4).

In a previous study using human eyes after death,[15] the density of I pores was positively correlated with the volume and duration of fixative perfusion, but the density of B pores showed no such correlation. In the present study no statistically significant correlation was observed between *volume* of fixative perfused and pore densities, for either I or B pores. However, there was a statistically significant positive correlation between I pore density and *duration* of fixative perfusion in ECA eyes (P = 0.027 by linear regression of log-transformed data). A similar correlation with duration of fixative perfusion existed in control eyes but just failed to reach statistical significance (P = 0.060 by linear regression of log-transformed data). There was relatively little variation in the duration of fixative perfusion in these eyes (range, 45 to 63 minutes for both experimental and control eyes), which may explain the lack of statistical significance seen in the control eyes. There was a larger variation in the range of fixative volumes perfused (experimental eyes, 78.3-647 μl; control eyes, 41-299 μl).

Platelets in Schlemm's Canal

Platelet aggregates were observed adhering to the inner wall in both control and ECA-perfused eyes. The aggregates varied greatly in appearance and size: Many aggregates were very small, consisting of no more than six or seven platelets, some were huge, incorporating many thousands of platelets (or more). The density of the platelet aggregates also varied: some were extremely dense, with no interplatelet spaces evident, whereas others appeared relatively open. Platelets in most aggregates were rounded or elliptical. Ethacrynic acid had a large effect on the number of such aggregates, causing a 158% increase in the number of aggregates per unit inner wall area (P < 0.0001) and a 210% increase in the percentage of the inner wall area covered by platelets (P = 0.012; Table 1). By TEM, platelets were seen to be covering focal openings in the inner wall of Schlemm's canal. Because of the relatively small number of samples studied by TEM and the difficulty of serially sectioning through the inner wall to find platelet aggregates, it was not possible to document the interaction between platelets and inner wall openings more extensively. For example, we did not determine the size of the openings covered by platelets, nor whether the platelets were covering B pores, I pores, or openings of unknown origin. The platelets appeared fairly densely packed near the inner wall openings, but it was

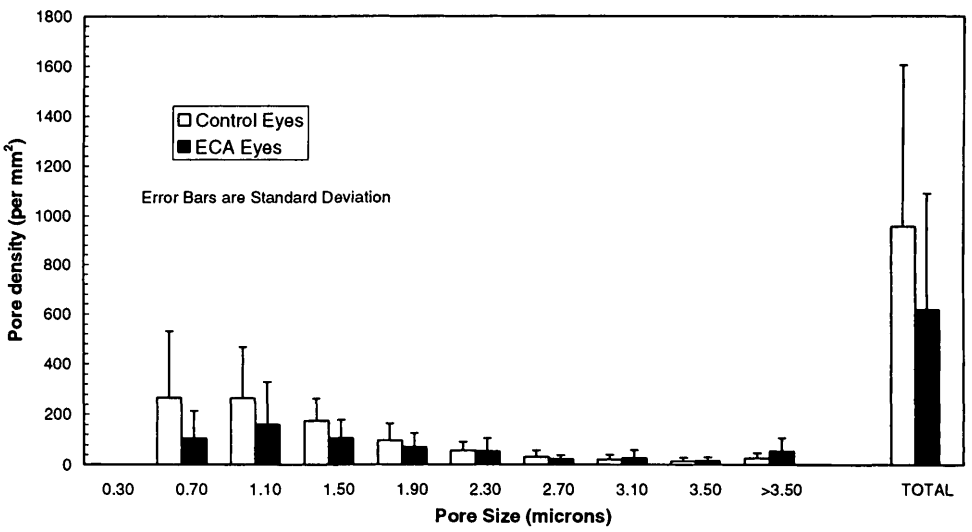

FIGURE 3. Pore size distribution for I pores in ECA-perfused and contralateral vehicle-perfused monkey eyes (n = 8 pairs).

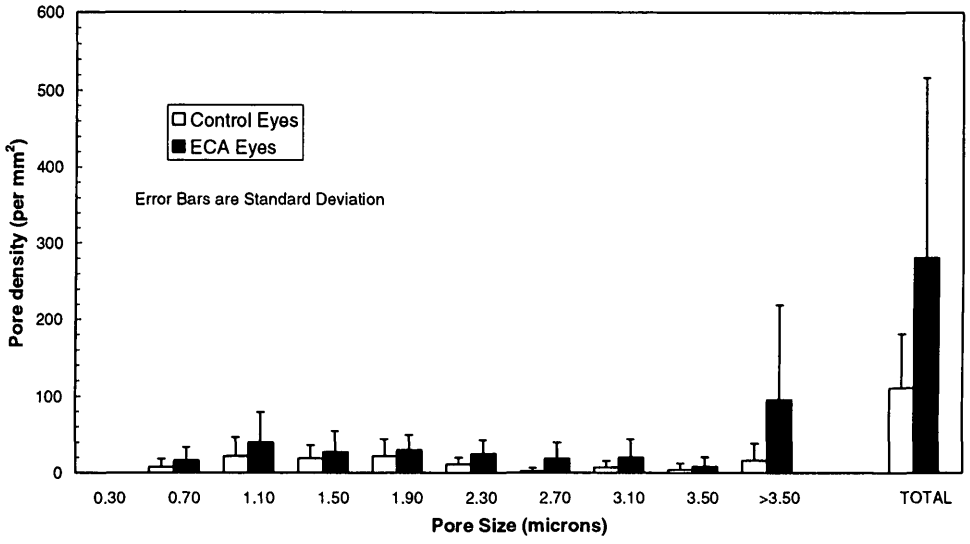

FIGURE 4. Pore size distribution for B pores in ECA-perfused and contralateral vehicle-perfused monkey eyes (n = 8 pairs).

not possible to estimate whether the overlying platelet aggregate was impermeable to fluid.

Relation between Facility and Inner Wall Pore Statistics

To determine whether inner wall pore statistics were correlated with facility, posttreatment facility in the control and ECA-treated groups was linearly regressed against pore density for each of B pores, B pores with sizes 1.9 μm or more, I pores and total pores, and against nD product for each of B pores, I pores, and total pores. We also regressed the overall facility ratio (C_{post}/C_{pre} for ECA-treated eyes divided by C_{post}/C_{pre} for contralateral control eyes) against pore density and nD product ratios (ECA/control) for B pores, I pores and T pores. No statistically significant relations were found, with the exception that in ECA-treated eyes, facility was negatively correlated with I pores. Specifically, there was a weak negative correlation (P = 0.052) between posttreatment facility and I pore density (Table 4). Because I pores make up the bulk of total pores, this caused a negative correlation between posttreatment facility and total pore density (P = 0.071; Table 4). Similar regressions of posttreatment facility and overall facility ratio versus platelet aggregate counts and area covered by platelets yielded no statistically significant relationships.

DISCUSSION

In this study, living monkey eyes perfused intracamerally with ECA showed increased outflow facility, markedly increased platelet adhesion to the inner wall of Schlemm's canal, decreased I pore density, and a tendency to increased density of large B pores, although it is important to note this latter finding did not reach statistical significance. The net 63% increase in facility that we observed is of comparable magnitude to that seen in previous studies using living monkeys. Using 10-μl bolus injections of 2.5 mM ECA into the AC, Epstein et al.[17] observed a net facility increase of approximately 20%, shortly after drug infusion, whereas Croft et al.[12] observed an increase of 71% 1 hour after drug infusion. When published values are used for the volume of the monkey AC (~100 μl for cynomolgus,[23,24] 120-130 μl for rhesus[29,30]), such a bolus dose produces an intracameral ECA concentration of 0.20 to 0.25 mM. Any differences between facility increases seen in the present study and those seen in previous studies are probably caused by differences in delivery protocol: We used a two-needle AC exchange that gives a very well-mixed AC and a continuous drug infusion approach that maintains a constant intracameral drug concentration. These well-controlled perfusion conditions may also explain the small standard errors seen in the net facility increase data.

Interpretation of our morphologic findings requires consideration of the effects of ECA on inner wall pores and the interaction between inner wall pores and platelets. We believe that our morphometric data are most consistent with a model whereby ECA increases the size and density of B pores, which in turn causes increased platelet adhesion in an attempt to

TABLE 4. Dependence of Posttreatment Facility on Inner Wall Features in Monkey Eyes

Response	Predictor	Slope Estimate*	P†
Post-Treatment Facility	Pore density (for total pores)	−0.29 (−0.608-0.033)	0.0706
	Pore density (I pores only)	−0.35 (−0.713-0.004)	0.0520
Post-Treatment Facility	nD product‡ (for total pores)	−0.15 (−0.416-0.110)	0.2043
	nD product‡ (I pores only)	−0.27 (−0.636-0.088)	0.1139

* Slope estimates are mean for 8 pairs of eyes, with 95% confidence interval in parentheses.

† Statistics are based on the relationship between the log(response) and the log(predictor) controlling for a fixed drug effect and random monkey effects.

‡ nD product is pore density times pore diameter, theoretically predicted[16] to correlate with facility.

cover these large B pores. Support for this scenario comes from the following observations.

1. Ethacrynic acid in the living monkey eye has been previously observed to promote B pores (focal loss of cell-cell attachment).[17]
2. The presence of breaks or openings in the inner wall seems to promote focal platelet adhesion. For example, Hamanaka and Bill[19] reported that elevated IOP or massage of the eye, both of which generally increased inner wall pore density, markedly increased the number of platelet aggregations on the inner wall. Hamanaka and Bill also showed that platelets tend to cover large (rather than small) pores preferentially. Platelets covering inner wall breaks after pharmacologic manipulation were also observed by Svedbergh et al.[7]
3. In human eyes, ECA produces B pores that are, on average, somewhat larger than those seen in control eyes.[13]
4. Although ECA causes large facility increases of nearly identical magnitude in both monkey and human[13] eyes, human eyes demonstrated a fivefold increase in B pore density, unlike the modest 5% increase in B pore density seen in monkey eyes.

Assuming that the action of ECA on the inner wall endothelial cells in monkey eyes is similar to that in human eyes, this line of thought predicts that large B pores created by ECA in monkey eyes would be largely masked by platelets. Such masking of B pores does not occur in human eyes after death,[13] because of absence of blood circulation.

Activation and adhesion of platelets in ECA-treated monkey eyes can also explain I pore density differences between this study and the companion paper reporting human eyes after death.[13] Activated platelets covering the inner wall in monkey eyes would probably obscure both I and B pores; thus, the apparent density of both I and B pores after ECA perfusion would be expected to be smaller in monkey eyes than in human eyes. This is precisely what was observed: I pore density was reduced by 46% in monkey eyes and was essentially unchanged in human eyes after death.[13]

Comments on the Role of Platelets

We observed platelet aggregates adhering to the inner wall endothelium even in control eyes. This is consistent with the findings of Hamanaka and Bill,[19] who observed adhering platelet aggregates in eyes that had never been cannulated or otherwise experimentally manipulated. It thus seems likely that some amount of platelet adhesion to the inner wall of Schlemm's canal is the norm.

Could the increased number of platelets adhering to the inner wall of Schlemm's canal after ECA treatment be caused by a direct action of ECA on platelets? Ethacrynic acid is known to influence platelet aggregation but in an inhibitory fashion. Yokoyama et al.[31] showed that ECA suppressed in vitro platelet aggregation induced by the thromboxane A_2 agonist U-46619, whereas ECA administration in patients tends to decrease platelet aggregation[32] and has been linked to thrombocytopenia.[33] This further supports the contention that the increased aggregation of platelets on the inner wall of Schlemm's canal is a secondary response to the production of large B pores by ECA, rather than an ECA effect on the platelets themselves. It might even be hypothesized that inhibition of platelet aggregation helps ECA increase facility, because plugging of inner wall breaks by activated platelets could reduce facility.

It is not clear where the "additional" platelets seen in the ECA-treated eyes came from. In earlier experiments (not reported here) we used different fixation and euthanatization protocols that were not successful in preventing blood reflux into Schlemm's canal; in those eyes, the inner wall was extensively covered with formed elements (primarily red cells). In the present experiments, we therefore used a protocol designed to avoid, as much as possible, immediate *antemortem* and *postmortem* reflux of blood into Schlemm's canal. Furthermore, care was taken to maintain an IOP greater than or equal to spontaneous IOP during the course of the experiment, so that IOP always exceeded episcleral venous pressure, and there was uninterrupted flow from the external reservoir into the eye and presumably through the outflow pathway. We occasionally saw formed elements (other than platelets) in Schlemm's canal, but because this was relatively unusual, we conclude that our strategy for preventing reflux was largely successful. Perhaps the platelets normally present in Schlemm's canal dispersed to create additional adhering aggregates in the ECA-treated eyes, or perhaps some entry of blood into Schlemm's canal is inevitable no matter how carefully the experiment is performed. Resolution of this issue would require further experimentation.

Relationship between Facility and Inner Wall Pores

The presence of platelet aggregates putatively covering inner wall openings in both ECA-treated and control eyes complicates the analysis of how inner wall pores do or do not influence facility. The effectiveness of platelets in occluding inner wall openings is uncertain; some aggregates appeared rather dense and may have been completely impermeable to fluid, whereas others appeared less so. Also, it is possible that some of the larger platelet aggregates covered more than one inner wall opening. Analysis of the relationship between inner wall pores and facility is also complicated by the dependence of inner wall pore density on the duration of fixation. This finding, which was previously observed in human eyes,[15] indicates that the fixation process itself is modifying inner wall pores. The fact that this dependence on fixation duration occurred in living monkey eyes suggests that the unknown process responsible for this effect is not caused by changes after death. This fact, and the masking of pores by platelets, means that the in vivo pore density is not known with any certainty. Further investigation is important to better understanding of the in vivo state of the inner wall of Schlemm's canal.

Given these uncertainties, it is perhaps not surprising that facility was not generally correlated with morphometric features of the inner wall. The one exception to this rule—namely, the negative correlation between facility and I pore density seen in ECA eyes—remains unexplained. Because such a correlation was not observed in control eyes, and because I pore density was decreased by ECA treatment, it is possible that activated platelets in ECA-treated eyes more aggressively covered all pore types, including I pores. In this scenario, ECA creates more large B pores, which activates platelets, and activated platelets cover some I pores, resulting in a net decrease in density of I pores. Another possibility is that aqueous humor drainage was redirected to a few preferential channels

after ECA administration, so that the overall pressure difference across the inner wall was reduced in most locations, leading to a decrease in I pore density. Although not definitive, we believe that our data in human eyes[13] argue against this possibility, as follows. Facility changes were similar in monkey and human eyes. If ECA were causing preferential flow channeling and subsequent reduction of I pores, we would have expected to see fewer I pores in human ECA eyes. However, this was not observed (companion paper,[13] Table 3). We therefore believe that masking of I pores by activated platelets in ECA-treated eyes is most consistent with our data, although it has not been definitively proved.

How does ECA increase outflow facility? Among several possibilities, we see two scenarios that merit further consideration: Either ECA acts on the inner wall endothelium to increase the number of B pores, or it weakens cell-extracellular matrix attachments in the JCT, leading to greater-than-normal washout of resistive material from the JCT. Observation supporting these hypotheses are summarized below:

1. Support for an inner wall mechanism: The most obvious ECA-induced morphologic change that could explain a facility increase remains the increased density of large inner wall B pores. This is consistent with early studies,[17] in which inner wall breaks observed by TEM were thought to be related to ECA's facility-increasing mechanism. In addition, previous work[17] did not note any distension of the JCT that would be expected to follow cell-matrix dissociation in ECA-treated eyes.
2. Support for a JCT mechanism: No correlation between inner wall pores and outflow facility was observed. This would definitively eliminate the inner wall mechanism, except that there are significant uncertainties about the in vivo pore distributions, for reasons discussed earlier.

We conclude that available data do not definitively support either scenario. It may be possible to gain evidence supporting one of these scenarios by studying the number and size of inner wall openings underlying platelet aggregates. Unfortunately, this would have to be done by TEM, and obtaining enough sections through platelet aggregates and openings to have a statistically representative sample would be remarkably difficult.

Recently, it has been proposed that ECA acts by promoting dephosphorylation of the cytoskeletal linkage protein focal adhesion kinase, which in turn alters F-actin and, ultimately, cell shape.[34] In this model, ECA weakens cell-extracellular matrix attachments (rather than cell-cell attachments), which causes inner wall cells to deform more in response to pressure or other stresses, thus leading to decreased intercellular attachment (increased paracellular flow). If loss of cell-substrate attachment was leading to increased deformation of inner wall cells in ECA-perfused eyes, we would expect to see larger giant vacuoles and more prominent distensions in ECA-perfused eyes than in control eyes. Our qualitative impressions do not support this expectation: Both giant vacuoles and inner wall herniations[35] did not appear to be larger or more frequent in ECA-treated eyes. However, we must point out that it is difficult to assess the extent of deformation of an inner wall cell from a scanning electron micrograph, and it is not impossible that there were subtle differences between ECA-treated eyes and control eyes that we were unable to discern. Additionally, the cytoskeletal mechanism suggested by O'Brien et al.[34] could affect cells in the JCT, with consequent effects on facility, either directly or through secondary effects on the inner wall. It would be worthwhile to study this issue more carefully in the future, perhaps through use of light micrographic sections rather than scanning electron micrographs.

General Comments

It is of interest to compare overall pore density in our control rhesus monkey eyes with data gathered by other investigators (Table 2). Our overall density of approximately 900 pores/mm^2 is slightly lower but generally consistent with reported values for rhesus monkeys but is notably lower than that reported by Svedbergh[35] and Hamanaka and Bill[19] for cynomolgus and Japanese monkeys. This may reflect a species difference or could have arisen because of slightly different pore-counting techniques (see later discussion). Svedbergh, who reported the highest pore density, observed many more small pores (sizes <0.50 μm) than either we or Moseley et al.[36] observed. It may be remarked that our pore size distribution histograms are more consistent with observations in human eyes, where the median pore size is in the range of 0.5 to 0.7 μm.

When quoting pore densities in the inner wall, it is important to consider how the sample viewing and pore-counting techniques may influence the results. Moseley et al.[36] have discussed this point; in their work, the sample was not tilted to visualize pores potentially hidden by vacuoles or other topographic features of the inner wall, and they argue that this leads to an underestimation of pore density. We have used a similar approach, and the same comments apply to our results as well: Our pore counts would tend to underestimate inner wall pore density somewhat. However, we took care to align the inner wall of Schlemm's canal parallel to the viewing plane for both vehicle-treated and ECA-treated eyes, so that this effect should introduce no bias into the paired comparisons.

Finally, the role of fixation conditions on pore density must be considered. Although we saw a dependence of pore density on fixation conditions, there were important differences between the present results in monkeys and the situation in human eyes.[13,15] For example, in monkey eyes, no dependence on fixative volume was seen, whereas such a dependence was observed in human eyes. We cannot explain these differences and speculate that they may be caused by the relatively small range of fixative volumes and durations used in the present study, by interspecies differences, and possibly by in vivo versus postmortem experimental conditions. Better understanding of how fixation conditions affect inner wall pores may aid in determining the physiology of the inner wall of Schlemm's canal.

References

1. Mäepea O, Bill A. The pressures in the episcleral veins, Schlemm's canal and the trabecular meshwork in monkeys: effects of changes in intraocular pressure. *Exp Eye Res.* 1989;49:645-663.
2. Mäepea O, Bill A. Pressures in the juxtacanalicular tissue and Schlemm's canal in monkeys. *Exp Eye Res.* 1992;54:879-883.
3. Ethier CR, Coloma FM, deKater AW, Allingham RR. Retroperfusion studies of the aqueous outflow system, Part II: studies in Human Eyes. *Invest Ophthalmol Vis Sci.* 1995;36:2466-2475.
4. Bill A, Svedbergh B. Scanning electron microscopic studies of the trabecular meshwork and the canal of Schlemm: an attempt to localize the main resistance to outflow of aqueous humor in man. *Acta Ophthalmol (Copenh).* 1972;50:295-320.

5. Grierson I, Lee WR. Pressure induced changes in the ultrastructure of the endothelial lining of Schlemm's canal. *Am J Ophthalmol.* 1975;81:863-884.
6. Svedbergh B. Effects of artificial intraocular pressure elevation on the outflow facility and the ultrastructure of the chamber angle in the vervet monkey (Cercopithecus ethiops). *Acta Ophthalmol (Copenh).* 1974;52:829-846.
7. Svedbergh B, Lütjen-Drecoll E, Ober M, Kaufman PL. Cytochalasin B-induced structural changes in the anterior ocular segment of the cynomolgus monkey. *Invest Ophthalmol Vis Sci.* 1978;17:718-734.
8. Kaufman PL, Erickson KA. Cytochalasin B and D dose-outflow facility response relationships in the cynomolgus monkey. *Invest Ophthalmol Vis Sci.* 1982;23:646-650.
9. Lindenmayer JM, Kahn MG, Hertzmark E, Epstein DL. Morphology and function of the aqueous outflow system in monkey eyes perfused with sulfhydryl reagents. *Invest Ophthalmol Vis Sci.* 1983;24:710-717.
10. Hamanaka T, Bill A. Morphological and functional effects of Na_2EDTA on the outflow routes for aqueous humor in monkeys. *Exp Eye Res.* 1987;44:171-190.
11. Hamanaka T, Bill A. Effects of alpha-chymotrypsin on the outflow routes for aqueous humor. *Exp Eye Res.* 1988;46:323-341.
12. Croft M, Hubbard WC, Kaufman PL. Effect of ethacrynic acid on aqueous outflow dynamics in monkeys. *Invest Ophthalmol Vis Sci.* 1994;35:1167-1175.
13. Ethier CR, Coloma FM. Effects of ethacrynic acid on Schlemm's canal inner wall and outflow facility in human eyes. *Invest Ophthalmol Vis Sci.* 1999;40:1599-1607.
14. Sit AJ, Coloma FM, Ethier CR, Johnson M. Factors affecting the pores of the inner wall of Schlemm's canal. *Invest Ophthalmol Vis Sci.* 1997;38:1517-1525.
15. Ethier CR, Coloma FM, Sit AJ, Johnson M. Two pore types in the inner-wall endothelium of Schlemm's canal. *Invest Ophthalmol-Vis.Sci.* 1998;39:2041-2048.
16. Johnson M, Shapiro A, Ethier CR, Kamm RD. The modulation of outflow resistance by the pores of the inner wall endothelium. *Invest Ophthalmol Vis Sci.* 1992;33:1670-1675.
17. Epstein DL, Freddo TF, Bassett-Chu S, Chung M, Karageuzian L. Influence of ethacrynic acid on outflow facility in the monkey and calf eye. *Invest Ophthalmol Vis Sci.* 1987;28:2067-2075.
18. Liang LL, Epstein DL, de Kater AW, Shahsafaei A, Erickson-Lamy KA. Ethacrynic acid increases facility of outflow in the human eye in vitro. *Arch Ophthalmol.* 1992;110:106-109.
19. Hamanaka T, Bill A. Platelet aggregation on the endothelium of Schlemm's canal. *Exp Eye Res.* 1994;59:249-256.
20. Bárány EH. Simultaneous measurements of changing intraocular pressure and outflow facility in the vervet monkey by constant pressure infusion. *Invest Ophthalmol.* 1964;3:135-143.
21. Kaufman PL, Bárány EH. Loss of acute pilocarpine effect on outflow facility following surgical disinsertion and retrodisplacement of the ciliary muscle from the scleral spur in the cynomolgus monkey. *Invest Ophthalmol.* 1976;15:793-807.
22. Bill A, Hellsing K. Production and drainage of aqueous humor in the cynomolgus monkey (Macaca irus). *Invest Ophthalmol.* 1965; 4:920-926.
23. Erickson KA, Gonnering RS, Kaufman PL, Dortzbach RK. The cynomolgus monkey as a model for orbital research, III:effects on ocular physiology of lateral orbitotomy and isolation of the ciliary ganglion. *Curr Eye Res.* 1984;3:557-564.
24. Erickson-Lamy K, Kaufman PL, McDermott ML, France NK. Comparative anesthetic effects on aqueous humor dynamics in the cynomolgus monkey. *Arch Ophthalmol.* 1984;102:1815-1820.
25. Kaufman PL, Bárány EH. Cytochalasin B reversibly increases outflow facility in the eye of the cynomolgus monkey. *Invest Ophthalmol Vis Sci.* 1977;16:47-53.
26. Kiland JA, Peterson JA, Gabelt BT, Kaufman PL. Effect of DMSO and exchange volume on outflow resistance washout and response to pilocarpine during anterior chamber perfusion in monkeys. *Curr Eye Res.* 1997;16:1215-1221.
27. Johnstone M, Tanner D, Chau B, Kopecky K. Concentration-dependent morphologic effects of cytochalasin B in the aqueous outflow system. *Invest Ophthalmol Vis Sci.* 1980;19:835-841.
28. Allingham RR, deKater AW, Ethier CR, Anderson PJ, Hertzmark E, Epstein DL. The relationship between pore density and outflow facility in normal and glaucomatous human eyes. *Invest Ophthalmol Vis Sci.* 1992;33:1661-1669.
29. Johnson SB, Passmore JA, Brubaker RF. The fluorescein distribution volume of the anterior chamber. *Invest Ophthalmol Vis Sci.* 1977;16:633-636.
30. Pederson JE, Gaasterland DE, MacLellan HM. Anterior chamber volume determination in the rhesus monkey. *Invest Ophthalmol Vis Sci.* 1978;17:784-787.
31. Yokoyama K, Kudo I, Nakamura H, Inoue K. A possible role for extracellular bicarbonate in U-46619-induced rat platelet aggregation. *Thromb Res.* 1994;74:369-376.
32. Savenkov MP. (Change in rheographic properties of blood in congestive circulatory insufficiency treated with diuretics.) Izmenenie reologicheskikh svoistv krovi u bol'nykh s zastoinoi nedostatochnost'iu krovoobrashcheniia pri lechenii diuretikami. *Kardiologiia.* 1977;17:52-57.
33. O'Dwyer PJ, LaCreta F, Nash S, et al. Phase I study of thiotepa in combination with the glutathione transferase inhibitor ethacrynic acid. *Cancer Res.* 1991;51:6059-6065.
34. O'Brien ET, Kinch M, Harding TW, Epstein DL. A mechanism for trabecular meshwork cell retraction: ethacrynic acid initiates the dephosphorylation of focal adhesion proteins. *Exp Eye Res.* 1997; 65:471-783.
35. Svedbergh B. Protrusions of the inner wall of Schlemm's canal. *Am J Ophthalmol.* 1976;82:875-882.
36. Moseley H, Grierson I, Lee WR. Mathematical modelling of aqueous humor outflow from the eye through the pores in the lining endothelium of Schlemm's canal. *Clin Phys Physiol Meas.* 1983; 4:47-63.
37. Bill A. Scanning electron microscopic studies of the canal of Schlemm. *Exp Eye Res.* 1970;10:214-218.